FEBS Letters 586 (2012) 3986–3990

FEBS Letters

journal homepage: www.FEBSLetters.org

Recognition of the let-7g miRNA precursor by human Lin28B

P. Shaik Syed Ali [a,*], Umesh Ghoshdastider [a,c], Jan Hoffmann [b], Bernd Brutschy [b], Slawomir Filipek [c]

[a] Institute of Biophysical Chemistry, Goethe University, Max-von-Laue-Str. 9, Frankfurt 60438, Germany
[b] Institute of Physical and Theoretical Chemistry, Goethe University, Max-von-Laue-Str. 7, Frankfurt 60438, Germany
[c] Faculty of Chemistry, University of Warsaw, ul. Pasteura 1, Warsaw 02-093, Poland

ARTICLE INFO

Article history:
Received 9 July 2012
Revised 9 September 2012
Accepted 26 September 2012
Available online 11 October 2012

Edited by Tamas Dalmay

Keywords:
Lin28B
Let-7g
Pre-miRNA

ABSTRACT

Mammalian homologs of lin28: Lin28 and Lin28B block the post-transcriptional processing of the let-7 family of miRNAs. We report that *in vitro* the terminal stem-loop region of the let-7g miRNA precursor (pre-let-7g) required to bind Lin28B is restricted to 24 nucleotides (nt) including the 3′ GGAG motif. Additionally, full length Lin28B is required for efficient binding to pre-let-7g and the stoichiometry of the complex is 1:1. Molecular dynamics (MD) simulations reveal the interactions of the pre-let-7g stem-loop and the GGAG motif in the stem region to the cold shock domain (CSD) and to the zinc knuckle domain (ZKD) of Lin28B, respectively.

1. Introduction

miRNAs are ~22 nt long non-coding RNAs, found in most eukaryotes including plants and animals, and were discovered around a decade ago [1]. miRNAs control most cellular processes, and are involved in gene silencing by directing RNA interference (RNAi) machinery through complementary base pairing to mRNAs [2]. They represent ~1% of all genes in the human genome with ~300 members, which are thought to regulate the expression of nearly one-third of all genes by RNAi, a highly conserved RNA guided gene silencing mechanism. Transcription factors are among the most commonly regulated targets of miRNAs, consistent with the roles of these small RNAs in cell differentiation [3,4]. There is also a close link between miRNA up and down regulation with certain cancers including breast cancer [5,6].

miRNA biogenesis is a multi-step process occurring in the nucleus and in the cytoplasm. From the primary transcript hairpin RNA (pri-miRNA), the microprocessor complex comprising RNAase III enzyme Drosha (Pasha in case of invertebrates) and DGCR8 (DiGeorge syndrome critical region 8 gene) cleaves the pri-miRNA hairpin into a hairpin of approximately 70 nt long precursor miRNA (pre-miRNA) [7,8]. The pre-miRNA is then exported from the nucleus into the cytoplasm by the membrane protein complex Exportin-5:Ran:GTP [9]. There it is processed by the enzyme Dicer into a 21–25 nt long double stranded miRNA and is loaded into the RNA induced silencing complex (RISC) [10,11]. In the RISC, the miRNA* strand is cleaved leaving the guide miRNA strand bound to the RISC [7]. Recognition of mRNA by the nucleoprotein complex with the incorporated miRNA strand leads to the cleavage of the target mRNA, or the repression of protein translation [12].

Lin28 regulates let-7 miRNA biogenesis, acting as a competitive inhibitor of Drosha mediated let-7 pri-miRNA [13] and Dicer mediated let-7 pre-miRNA processing [14]. The mammalian homologs of lin28 are Lin28 and Lin28B. Human Lin28B is a protein of 250 amino acids. Comparison of mammalian Lin28B sequences shows that the protein is highly conserved, with nearly 85% identity with mouse and 36% identity with *Caenorhabditis elegans*. Lin28 proteins contain a cold shock domain (CSD) followed by two consecutive CCHC type zinc finger domains forming a zinc knuckle domain (ZKD) [15]. Although these folds are found ubiquitously in nature, the arrangement of the CSD with the ZKD is unique to Lin28 in animals.

Lin28's role in cell differentiation is underscored by a number of recent findings in *C. elegans* [3,4]. Lin28/Lin28B specifically regulates members of the let-7 family of miRNAs in humans that include let-7a to let7i, and the close relative miR98. The let-7 miRNA, based on genetic experiments in *C. elegans*, is involved in developmental timing [3,4]. Additionally, let-7 miRNA regulates oncogenes (Ras, c-Myc, HMGA-2) and cell-cycle genes (Cyclin D1, D2, Cdc25a and Cdk6). More recent studies have shown that the level of mature let-7 is directly correlated with the expression levels of Lin28/Lin28B. Other investigators have shown that overexpression of Lin28/Lin28B occurs in a wide variety of human

* Corresponding author. Fax: +49 69 798 29632.
E-mail address: shaikpakeer@gmail.com (P. Shaik Syed Ali).

0014-5793/$36.00
http://dx.doi.org/10.1016/j.febslet.2012.09.034

cancers, coupled with depressed levels of mature let-7 [16]. Recent evidence suggests that Lin28 can modulate the translation of mRNAs required for cell growth, metabolism, stem cells, metabolic diseases and cancer [17]. Therefore, Lin28/Lin28B can be used as a marker for various tumors.

Lately, the crystal structure of mouse Lin28 bound to the let-7 family of RNAs has been reported [15]. Furthermore, the crystal structures of apo human and *Xenopus tropicalis* (Xtr) Lin28B CSD with hexa, hepta thymidine [18], and the NMR structure of the Lin28 ZKD with let-7 fragment comprising the GGAG motif [19] have been solved. However the minimal length of pre-let-7g RNA required for binding to Lin28B and the stoichiometry of the complex are unknown. In this paper we demonstrate by truncations of Lin28B that full length Lin28B is required to bind efficiently to pre-let-7g. Furthermore, we reveal the minimal length of pre-let-7g required for the binding to Lin28B and that the stoichiometry of the complex is 1:1. MD simulations identify the residues of Lin28B involved in binding to pre-let-7g.

2. Results and discussion

2.1. Minimal length of pre-let-7g required for binding to Lin28B is 24 nt

Human Lin28 has been demonstrated to bind to the 40 nt long terminal stem-loop of pre-let-7g [20]. The minimal length of pre-let-7g that interacts with Lin28B has yet to be determined. The interactions of the full length Lin28B (residues 1–250) binding to the 5′-end ^{32}P labeled 28 nt, 24 nt and 20 nt long pre-let-7g RNA constructs, which preserve the terminal stem-loop were analyzed by electrophoretic mobility shift assay (EMSA) (Fig. 1). EMSA experiments were performed with $\sim 1 \times 10^5$ cpm of 5′-end ^{32}P labeled pre-let-7g 28 nt, 24 nt that includes the GGAG motif at the 3′ end and a 20 nt RNA lacking nucleotides AG of the GGAG motif, which were titrated to full length Lin28B, protein concentrations ranging from 60 nM to 16 μM. Full length Lin28B showed a clear gel shift indicative of complex formation with 28 nt (Fig. 1A) and 24 nt (Fig. 1B) but not with 20 nt long pre-let-7g (Fig. S1A).

Lin28B selective binding to the 24 nt long pre-let-7g but not to the shorter length RNA suggests that though the terminal stem-loop of let-7g may be essential to bind Lin28 [15], a few nucleotides in the stem region, within the terminal stem-loop of pre-let-7g play a crucial role in the binding of Lin28B to pre-let-7g. The GGAG motif is a common motif among the let-7 RNAs (21), with the first and last G of GGAG thought to be the key interactions (19). However the absence of last G from GGAG completely abolished the binding of Lin28B to pre-let-7g that was observed in 20 nt RNA (Fig. S1A). Therefore, no region beyond the 24 nt of pre-let-7g RNA is required to bind Lin28B and binding to this region may be sufficient to inhibit the access of Dicer to block the let-7g miRNA biogenesis.

2.2. Full-length Lin28B is required for efficient binding to pre-let-7g

In order to assess the relative contributions of the Lin28B domains in recognizing pre-let-7g, truncated versions of Lin28B were expressed, and binding to $\sim 1 \times 10^5$ cpm of 5′-end ^{32}P labeled pre-let-7g RNA constructs was analyzed by EMSA (Fig. 1). Full-length Lin28B titrated with 28 nt and 24 nt pre-let-7g, formed complexes (Fig. 1). A second construct was created, residues 29–176, preserving both the CSD and the ZKD. This truncated construct still bound 24 nt pre-let-7g, albeit with a significantly reduced affinity. In a titration from 250 nM to 16 μM, 29–176 shows a distinct gel shift, but no saturation, even at 16 μM protein concentration (Fig. 1C). The binding of the truncated ZKD (residues 127–176) to 24 nt

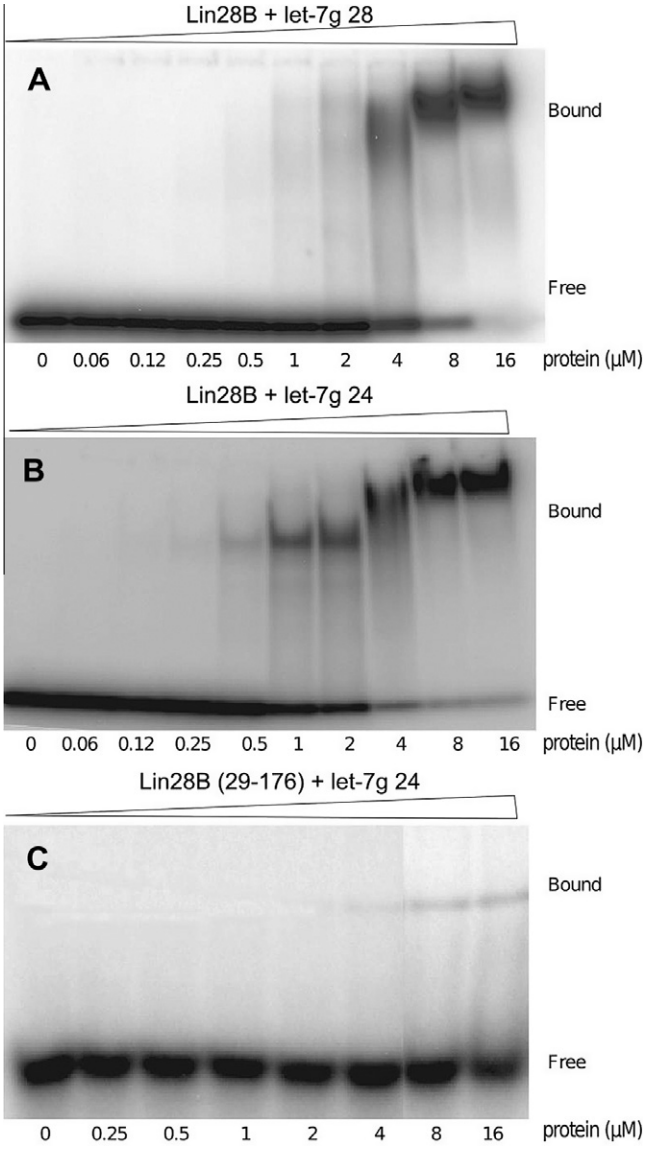

Fig. 1. Lin28B interaction with pre-let-7g RNA. (A) Gel shift experiments carried out with $\sim 1 \times 10^5$ cpm of 5′-end ^{32}P labeled 28 nt pre-let-7g with indicated concentrations of full length Lin28B. (B) Gel shift experiments carried out with $\sim 1 \times 10^5$ cpm of 5′-end ^{32}P labeled 24 nt pre-let-7-g with indicated concentrations of full length Lin28B. (C) Gel shift experiments carried out with $\sim 1 \times 10^5$ cpm of 5′-end ^{32}P labeled 24 nt pre-let-7g with indicated concentrations of Lin28B 29–176 (CSD and ZKD).

pre-let-7g was also conducted. The ZKD did not show any appreciable binding to 24 nt pre-let-7g (Fig. S1B). The binding of the truncated CSD (29–101) could not be tested as it was not soluble. These results demonstrate that the ZKD alone could not interact to pre-let-7g. However the full length protein shows stronger interaction to pre-let-7g compared to the truncate residues 29–176 that contains the CSD and the ZKD. Therefore, the full-length protein is required for high affinity binding. The contribution of the remaining amino acids upstream and downstream the CSD and the ZKD are required and may be involved in stabilizing the domains relative to one another for efficient binding.

2.3. Stoichiometry of the Lin28B:pre-let-7g complex is 1:1

The truncated CSD and ZKD construct of mouse Lin28 showed a 1:1 stoichiometric complex with pre-let-7d RNA (15). Analytical

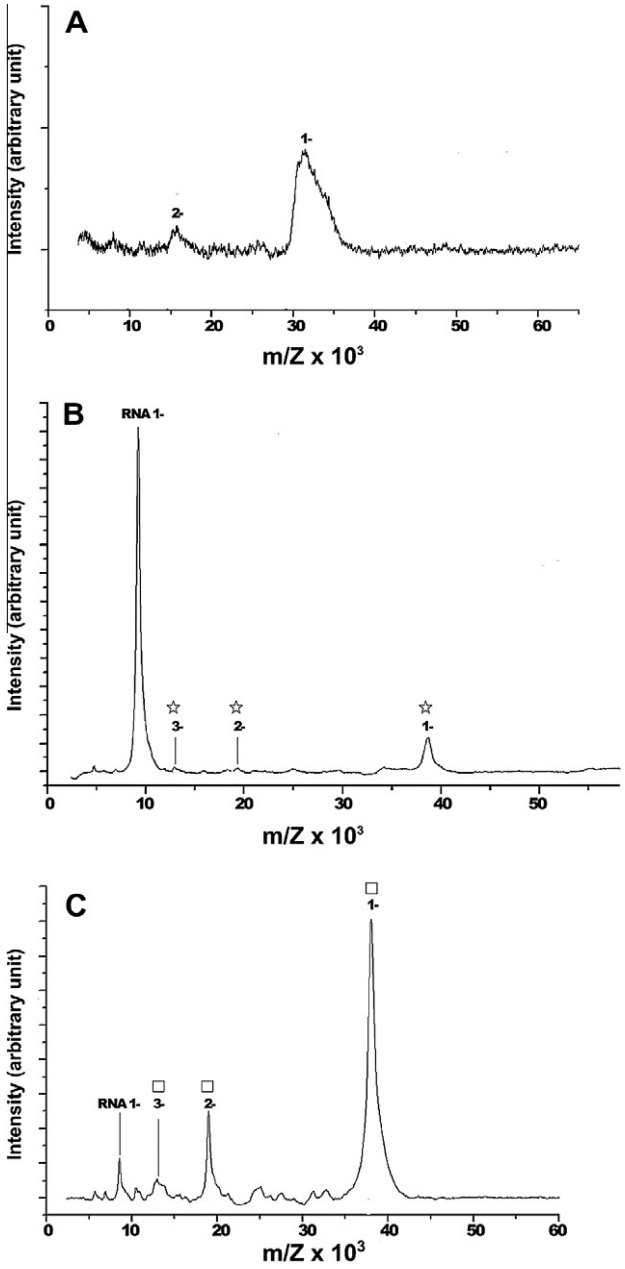

Fig. 2. LILBID mass spectra of full length Lin28B alone and the full length Lin28B in the presence of 28 nt and 24 nt pre-let-7g RNA. (A) Mass spectrum showing full length Lin28B as a monomer with a mass corresponding to ~29.1 kDa. (B) Mass spectrum of full length Lin28B and pre-let-7g 28 incubated in 1:1 ratio (~5 μM:5 μM). Star represents 1:1 stoichiometric complex of full length Lin28B:pre-let-7g 28 with a mass corresponding to ~38.2 kDa. (C) Mass spectrum of full length Lin28B and pre-let-7g 24 incubated in 1:1 ratio (~5 μM:5 μM). Box represents 1:1 stoichiometric complex of full length Lin28B:pre-let-7g 24 with a mass corresponding to ~37.7 kDa.

gel filtration experiments showed a single peak of the full length Lin28B:pre-let-7g complex, with the free pre-let-7g RNA running as a monodispersed peak (Fig. S2). In order to determine the stoichiometry of the complex quantitatively, LILBID mass spectrometry method was used (Fig. 2), which is useful for measuring the mass of noncovalent protein complexes. This is a robust method, and has previously been used to identify interactions in the 30S and 50S subunits of the ribosome, interactions in membrane proteins such as the light harvesting complexes and also in protein:nucleic acid complexes [22].

The full length Lin28B protein, pre-let-7g 28 nt and 24 nt RNA showed masses of around ~29.1 kDa (Fig. 2A), ~9.1 kDa (Fig. S3A) and ~8.6 kDa (Fig. S3B), respectively. The estimated mass values of Lin28B protein and pre-let-7g 28 nt, 24 nt are nearly equivalent to the calculated corresponding amino acid and nucleic acid sequences. To determine the stoichiometry of full length Lin28B:pre-let-7g 28 and full length Lin28B:pre-let-7g 24 complex, the protein and RNA were mixed in equimolar ratio and screened.

The Lin28B:pre-let-7g 28 and Lin28B:pre-let-7g 24 complex peaks showed masses of ~38.2 kDa (Fig. 2B) and ~37.7 kDa (Fig. 2C), respectively. The estimated molecular masses of ~38.2 kDa and ~37.7 kDa are equal to that of a 1:1 complex of full length Lin28B:pre-let-7g 28 and Lin28B:pre-let-7g 24, respectively. These results demonstrate that Lin28B and pre-let-7g form a 1:1 complex. *In vitro*, the stoichiometry of the Lin28B:pre-let-7g complex is 1:1 and remains constant even with 10-fold excess molar ratio of pre-let-7g RNA to protein (Fig. S3C and D). This suggests that the RNA binding residues of Lin28B engage in binding a lone pre-let-7g and thus cannot bind additional RNA molecules, even at higher RNA concentrations. This may explain the absence of larger macro molecular complexes even at higher RNA concentrations (Fig. S3C). However, Lin28B shows comparatively weaker interactions with 28 nt pre-let-7g (Fig. 2B) than with 24 nt (Fig. 2C), which is evident from the elevated complex peak and correspondingly diminished RNA peak in the later.

2.4. MD simulation of Lin28B:pre-let-7g complex reveals the molecular interactions

An homology model of the Lin28B:pre-let-7g complex (Fig. 3A) obtained by aligning the Lin28B sequence to mouse Lin28 was used for a 40 ns long MD simulation in Gromacs [23] for checking of the stability of the modeled Lin28B:pre-let-7g. The ZKD of Lin28B interacted with pre-let-7g GGAG motif during and after the simulation. After the simulation, the first G of GGAG motif formed a pi stacking interaction with H152 of Lin28B corresponding to H162 in mouse Lin28 [15], and the last G was sandwiched between Y130 and H138 of Lin28B by pi stacking interactions, corresponding to Y140 and H148 in mouse Lin28 (Fig. 3B and C). The A of GGAG motif was found to be orienting to Y130 of Lin28B in order to optimize the pi stacking interaction, corresponding to Y140 in mouse Lin28 (Fig. 3C). Additionally, the first G was within H-bonding distance of K149, K150, H152, and V161 of Lin28B, corresponding to K159, K160, H162, and V171 in mouse Lin28. The second G and last G were involved in H-bonding interaction with K149 and Y130, R128, A139, and H138 of Lin28B, corresponding to K159 and R138, Y143, H148, and A149 in mouse Lin28, respectively (Fig. S4). Prolonged simulation of μs length could orient them even further. The residues of the ZKD involved in interactions with the GGAG motif are mostly preserved between mouse Lin28 and human Lin28B since they can be aligned (Fig. 3D). A previous report stated that Lin28 binding to pre-let-7g is abolished by C161A, F73A, F47A mutations that are involved in binding to let-7g, which is unlikely [20]. Moreover, the NMR structure of the ZKD in complex with isolated 5′-AGGAGU-3′ indicated that the 5′-NGNNG-3′ motif of let-7g is required for recognition by the ZKD, which is similar to our observation. Previously, the NMR structure of the HIV-1 nucleocapsid protein bound to stem-loop SL2 of the psi-RNA revealed that the second and fourth G of GGAG/GGUG motif are involved in binding the ZKD [24].

In our Lin28B model, each zinc atom forms a tetrahedral coordination complex with C129, C132, C142, H137 and C151, C154, C164, and H159 in the ZKD. In mouse Lin28, the corresponding residues are C161, C164, C174, H169 and C139, C142, C152, and H147, respectively. CCHC type ZKDs are found in nucleocapsid proteins of retroviruses playing a major role in packing of the genetic material

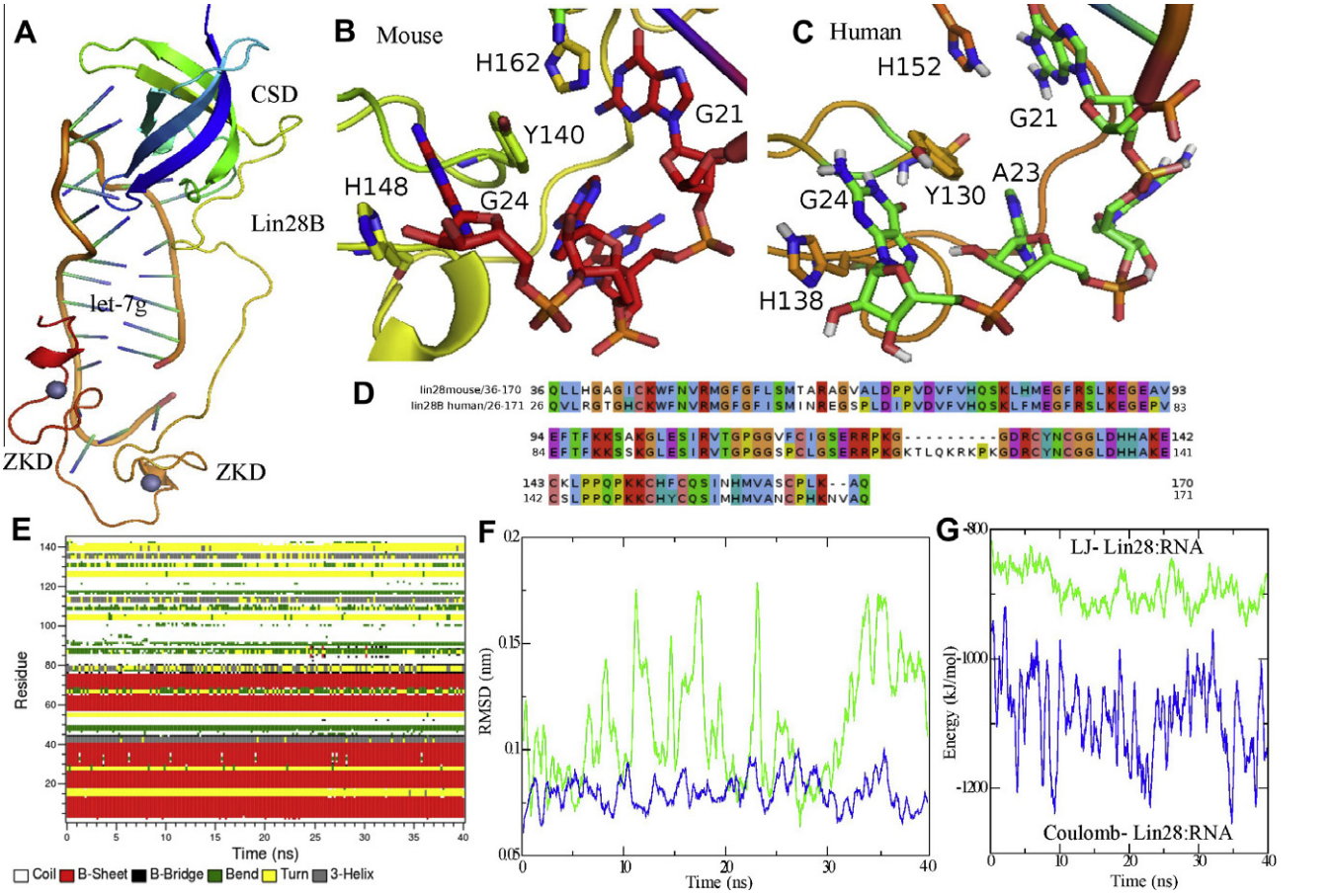

Fig. 3. MD simulations of human Lin28B:pre-let-7g complex. (A) pre-let-7g in complex with the homology model of Lin28B (based on the crystal structure of mouse Lin28:pre-let-7g (PDB ID: 3TS2)). (B) pi stacking interactions of mouse Lin28 with the GGAG motif. (C) pi stacking interactions of human Lin28B with the GGAG motif. (D) Sequence alignment of mouse Lin28 with human Lin28B used in the homology modeling. (E) Evolution of Lin28B secondary structure during MD simulation of the Lin28B:pre-let-7g complex. (F) RMSD of the CSD (shown in blue) and the ZKD (shown in green) during the 40 ns MD simulations. (G) Interaction energy between Lin28B and pre-let-7g during the simulation. Lennard–Jones (LJ)/van der Waals and electrostatic (Coulomb's) interaction energies are shown in green and blue, respectively.

early in the infection process. Mutations in the ZKD inhibit the 3'-terminal uridinylation of pre-let-7 RNAs and thus block the biogenesis of let-7 miRNAs [14,21]. This is in agreement with our simulations, where ZKD has no defined structure and it fails to bind to the let-7g GGAG motif in the absence of zinc, which prevents CCHC type zinc finger formation. The first and last G of the GGAG motif determine the key interactions (Figs. 3B, C and S4), and their mutation resulted in loss of binding, whereas the A of the GGAG motif hardly has any influence on binding [19].

The CSD (~75 amino acids) is conserved in prokaryotic and eukaryotic DNA binding proteins. The CSD is known to bind single stranded RNA and the structure of this domain has been conserved during evolution. Interactions of the CSD with pre-let-7g were also preserved in the case of human as observed for mouse. pre-let-7g G1-A13 in the stem loop is shown to interact with various residues of the CSD. After MD simulations, it was found that G2, G3, G4**, C6, U7, A8, G10, A11, U12, C15**, and A16 were involved in H-bonding and hydrophobic interactions with the Lin28B CSD, whereas U9 and A13 formed only hydrophobic contacts (Fig. S5). In the case of mouse Lin28, **C6, U7, A8,** U9, **G10, A11, U12, C15**, and A13 make H-bonding and hydrophobic contacts and A16 only has hydrophobic contacts (Fig. S5) (The common nucleotides are highlighted in bold). Interactions of G2, G3 and G4 to the CSD of Lin28B unlike mouse Lin28, could be pivotal in recognizing the pre-let-7g stem loop. As reported recently by Mayr et al. [18], the CSD is involved in remodeling of let-7 before binding to the ZKD and it acts as a molecular chaperone for RNA folding.

Secondary structure analysis indicates conservation in the simulation of the CSD beta sheet unlike the ZKD, which changes between turns, coils and bends (Fig. 3E). The complex was stable during the simulation as shown in the root mean square deviation (RMSD) plot (Fig. 3F). The RMSD of the CSD was within 1 Å throughout the simulation, whereas for the ZKD domain it varied between 0.5 and 1.5 Å due to the flexibility of the region, although its interactions with the GGAG motif were preserved (Fig. 3F). This flexibility facilitates the binding of Lin28B to the let-7 family of miRNAs, with a shorter or longer loop preceding the GGAG motif. Coulomb and Lennard Jones interaction energies between Lin28B and let-7g decreased from −950 to −1150 kJ/mol and −800 to −875 kJ/mol, respectively during the simulation (Fig. 3G). Root mean square fluctuation (RMSF) analysis points towards the flexibility of the CSD to be ~2 Å and that of the ZKD ~2–4 Å (Fig. 4A). During principal component analysis (PCA) from the MD simulations, the movement of the ZKD in upward direction was also observed, which will allow binding to the shorter length pre-let-7g with the conserved GGAG motif. Plotting the first Eigenvector of Lin28B to that of let-7g indicates that both motions are linearly correlated (Fig. 4B). NMR studies have led to the proposal that the flexibility of the linker is able to accommodate various let-7s to Lin28 [15].

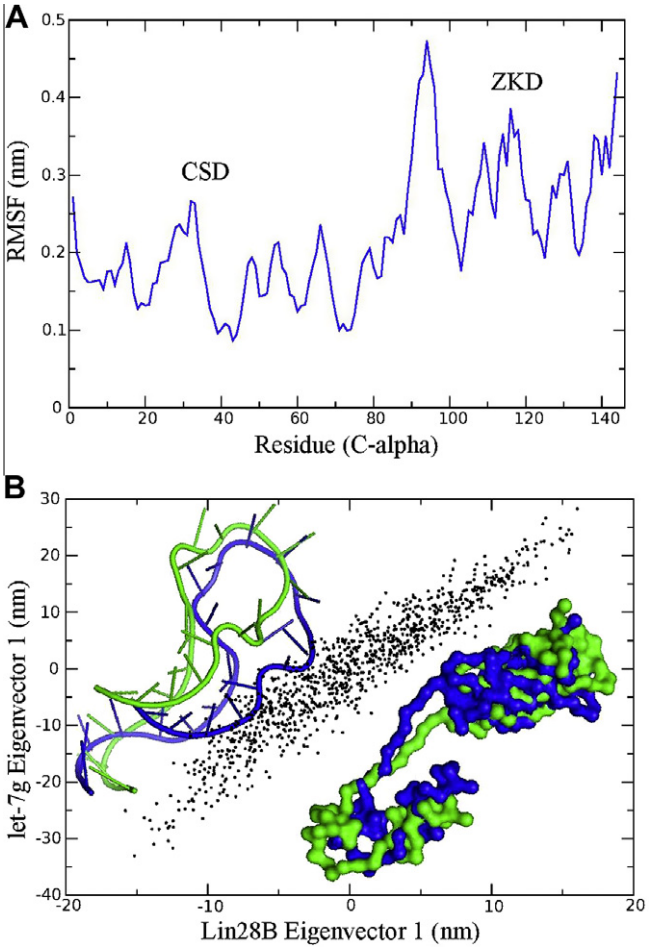

Fig. 4. (A) RMSF of Lin28B C-alpha atoms throughout the simulation. (B) Plot of the first Eigenvector obtained from the PCA of Lin28B and pre-let-7g motions, respectively. Direction of movement along the first eigenvector can be identified by the initial (in green) and final (in blue) position of Lin28B and pre-let-7g.

In this paper, we propose for the first time the minimal lengths of pre-let-7g and human Lin28B required for binding. The stoichiometry of the complex was determined to be 1:1. Based on MD simulations we show the Lin28B residues that are involved in the interaction with pre-let-7g.

3. Materials and methods

Materials and methods are described in supplementary information.

Acknowledgments

This work was funded by the Hessian Ministry of Science and Culture and the European Community's Seventh Framework Program (FP7/2007-2013) under Grant Agreement No. 211800 (UG). Support by Prof. Volker Dötsch (Institute of Biophysical Chemistry, Goethe University, Frankfurt) and Dr. Julian Chen is gratefully acknowledged. We also thank Dr. Robert Robinson, IMCB, Singapore for carefully proofreading the manuscript.

Appendix A. Supplementary data

Supplementary data associated with this article can be found, in the online version, at http://dx.doi.org/10.1016/j.febslet.2012.09.034.

References

[1] Lagos-Quintana, M., Rauhut, R., Lendeckel, W. and Tuschl, T. (2001) Identification of novel genes coding for small expressed RNAs. Science 294 (5543), 853–858.
[2] Krol, J., Loedige, I. and Filipowicz, W. (2010) The widespread regulation of microRNA biogenesis, function and decay. Nat. Rev. Genet. 11 (9), 597–610.
[3] Abbott, A.L., Alvarez-Saavedra, E., Miska, E.A., Lau, N.C., Bartel, D.P., Horvitz, H.R. and Ambros, V. (2005) The let-7 MicroRNA family members mir-48, mir-84, and mir-241 function together to regulate developmental timing in *Caenorhabditis elegans*. Dev. Cell 9 (3), 403–414.
[4] Reinhart, B.J., Slack, F.J., Basson, M., Pasquinelli, A.E., Bettinger, J.C., Rougvie, A.E., Horvitz, H.R. and Ruvkun, G. (2000) The 21-nucleotide let-7 RNA regulates developmental timing in *Caenorhabditis elegans*. Nature 403 (6772), 901–906.
[5] Johnson, S.M., Grosshans, H., Shingara, J., Byrom, M., Jarvis, R., Cheng, A., Labourier, E., Reinert, K.L., Brown, D. and Slack, F.J. (2005) RAS is regulated by the let-7 microRNA family. Cell 120 (5), 635–647.
[6] Takamizawa, J., Konishi, H., Yanagisawa, K., Tomida, S., Osada, H., Endoh, H., Harano, T., Yatabe, Y., Nagino, M., Nimura, Y., Mitsudomi, T. and Takahashi, T. (2004) Reduced expression of the let-7 microRNAs in human lung cancers in association with shortened postoperative survival. Cancer Res. 64 (11), 3753–3756.
[7] Gregory, R.I., Chendrimada, T.P. and Shiekhattar, R. (2006) MicroRNA biogenesis: isolation and characterization of the microprocessor complex. Methods Mol. Biol. 342, 33–47.
[8] Lee, Y., Ahn, C., Han, J., Choi, H., Kim, J., Yim, J., Lee, J., Provost, P., Rådmark, O., Kim, S. and Kim, V.N. (2003) The nuclear RNase III Drosha initiates microRNA processing. Nature 425 (6956), 415–419.
[9] Bohnsack, M.T., Czaplinski, K. and Gorlich, D. (2004) Exportin 5 is a RanGTP-dependent dsRNA-binding protein that mediates nuclear export of pre-miRNAs. RNA 10 (2), 185–191.
[10] Jaskiewicz, L. and Filipowicz, W. (2008) Role of Dicer in posttranscriptional RNA silencing. Curr. Top. Microbiol. Immunol. 320, 77–97.
[11] Hutvágner, G., McLachlan, J., Pasquinelli, A.E., Bálint, E., Tuschl, T. and Zamore, P.D. (2001) A cellular function for the RNA-interference enzyme Dicer in the maturation of the let-7 small temporal RNA. Science 293 (5531), 834–838.
[12] Hutvagner, G. and Simard, M.J. (2008) Argonaute proteins: key players in RNA silencing. Nat. Rev. Mol. Cell Biol. 9 (1), 22–32.
[13] Newman, M.A., Thomson, J.M. and Hammond, S.M. (2008) Lin-28 interaction with the Let-7 precursor loop mediates regulated microRNA processing. RNA 14 (8), 1539–1549.
[14] Heo, I., Joo, C., Cho, J., Ha, M., Han, J. and Kim, V.N. (2008) Lin28 mediates the terminal uridylation of let-7 precursor MicroRNA. Mol. Cell. 32 (2), 276–284.
[15] Nam, Y., Chen, C., Gregory, R.I., Chou, J.J. and Sliz, P. (2011) Molecular basis for interaction of let-7 microRNAs with Lin28. Cell 147 (5), 1080–1091.
[16] Viswanathan, S.R. and Daley, G.Q. (2010) Lin28: A microRNA regulator with a macro role. Cell 140 (4), 445–449.
[17] Huang, Y. (2012) A mirror of two faces: Lin28 as a master regulator of both miRNA and mRNA. Wiley Interdisciplinary Reviews. RNA 3 (4), 483–494.
[18] Mayr, F., Schütz, A., Döge, N. and Heinemann, U. (2012) The Lin28 cold-shock domain remodels pre-let-7 microRNA. Nucleic Acids Res. 40 (15), 7492–7506.
[19] Loughlin, F.E., Gebert, L.F.R., Towbin, H., Brunschweiger, A., Hall, J. and Allain, F.H.-T. (2011) Structural basis of pre-let-7 miRNA recognition by the zinc knuckles of pluripotency factor Lin28. Nat. Struct. Mol. Biol. 19 (1), 84–89.
[20] Piskounova, E., Viswanathan, S.R., Janas, M., LaPierre, R.J., Daley, G.Q., Sliz, P. and Gregory, R.I. (2008) Determinants of microRNA processing inhibition by the developmentally regulated RNA-binding protein Lin28. J. Biol. Chem. 283 (31), 21310–21314.
[21] Heo, I., Joo, C., Kim, Y.-K., Ha, M., Yoon, M.-J., Cho, J., Yeom, K.-H., Han, J. and Kim, V.N. (2009) TUT4 in concert with Lin28 suppresses microRNA biogenesis through pre-microRNA uridylation. Cell. 138 (4), 696–708.
[22] Rashid, U.J., Hoffmann, J., Brutschy, B., Piehler, J. and Chen, J.C.-H. (2008) Multiple targets for suppression of RNA interference by tomato aspermy virus protein 2B. Biochemistry 47 (48), 12655–12657.
[23] Hess, B., Kutzner, C., Van Der Spoel, D. and Lindahl, E. (2008) GROMACS 4: algorithms for highly efficient, load-balanced, and scalable molecular simulation. J. Chem. Theory Comp. 4 (3), 435–447.
[24] Amarasinghe, G.K., De Guzman, R.N., Turner, R.B., Chancellor, K.J., Wu, Z.R. and Summers, M.F. (2000) NMR structure of the HIV-1 nucleocapsid protein bound to stem-loop SL2 of the psi-RNA packaging signal. Implications for genome recognition. J. Mol. Biol. 301 (2), 491–511.